

## Introduction

Dipeptidyl peptidase III isolated from *Bacteroides thetaiotaomicron* (Bt-DPP3) is a two-domain zinc exopeptidase from M49 family. Members of this protease family, characterized by their HEXXGH and EEXR(K)AE(D) motifs, cleave dipeptidyl residues from the N-terminus of the substrate. They have been suggested to participate in pain modulation, defense against oxidative stress and intracellular protein catabolism. The crystallographic structure of Bt-DPP3 reveals two domains separated by a wide cleft, strongly resembling the 3D structure of its human ortholog despite the fairly low sequence identity (~23%).

The active site is composed from the Zn<sup>2+</sup> ion coordinated by two His and a Glu residue of the HEXXGH motive (His448, His 453 and Glu449, respectively), as well as by the Glu476 of the EEXRAD motive (Fig. 1). Computational studies performed on the human DPP3 show that the coordination number of Zn<sup>2+</sup> varies greatly over the course of 100 ns, and could be vital to understanding the reaction mechanism<sup>1</sup>. In this work the synthetic substrates Arg-Arg-2-naphtylamide (RRNA) and Lys-Ala-2-naphtylamide (KANA) were docked into the wild-type enzyme and the C450S mutant using the ff12SB and ff14SB force field.

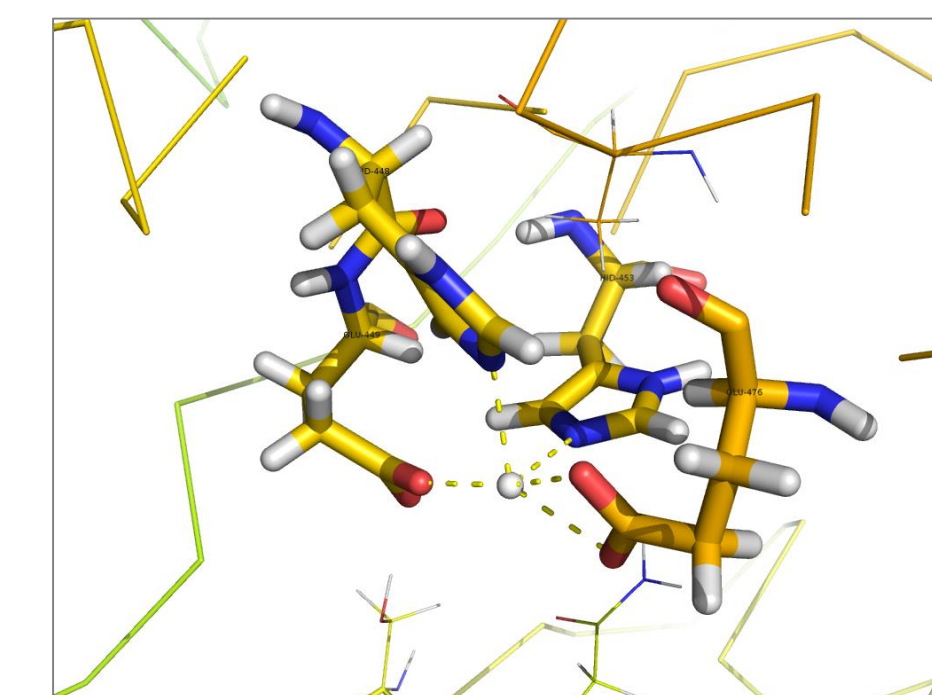


Figure 1. Active site of Bt-DPP3

## Methodology

All input geometries were based on the crystallographically determined “open” structure of Cys→Ser Bt-DPP3 mutant and the known structure of the human DPP III complex with tyrosin. Prior to MD simulations, the mutations have been reverted using tLeap and all systems have been optimized in three cycles with different constraints. Upon minimization, the structures have been gently heated from 0 to 300 K during a 50 ns period using the NVT ensemble, while the MD simulations were performed for 200 ns at 300 K and constant pressure (*NpT* ensemble). The temperature was held constant using Langevin thermostat with a collision frequency of 1 ps<sup>-1</sup>. All calculations were performed with AMBER program package using periodic boundary conditions, while the electrostatic interactions were calculated using the particle-mesh Ewald method. Bonds involving hydrogen atoms were constrained using the SHAKE algorithm. Ff12SB force field was used for classical MD, whereas the ff14SB force field was used in conjunction with accelerated MD<sup>2</sup>.

## Results

Both RRNA and KANA were successfully docked into the active site of DPP III. aMD seems to result in better substrate placement with classical MD providing structures with slightly higher energies. This can be a result of the naphthalene core entering deeper into the hydrophobic pocket (Figure 2.). Calculated energies are in good agreement with kinetically determined data<sup>3</sup>. The difference in calculated binding energies and experimentally determined relative hydrolysis rates can be explained through hydrogen bond analysis.

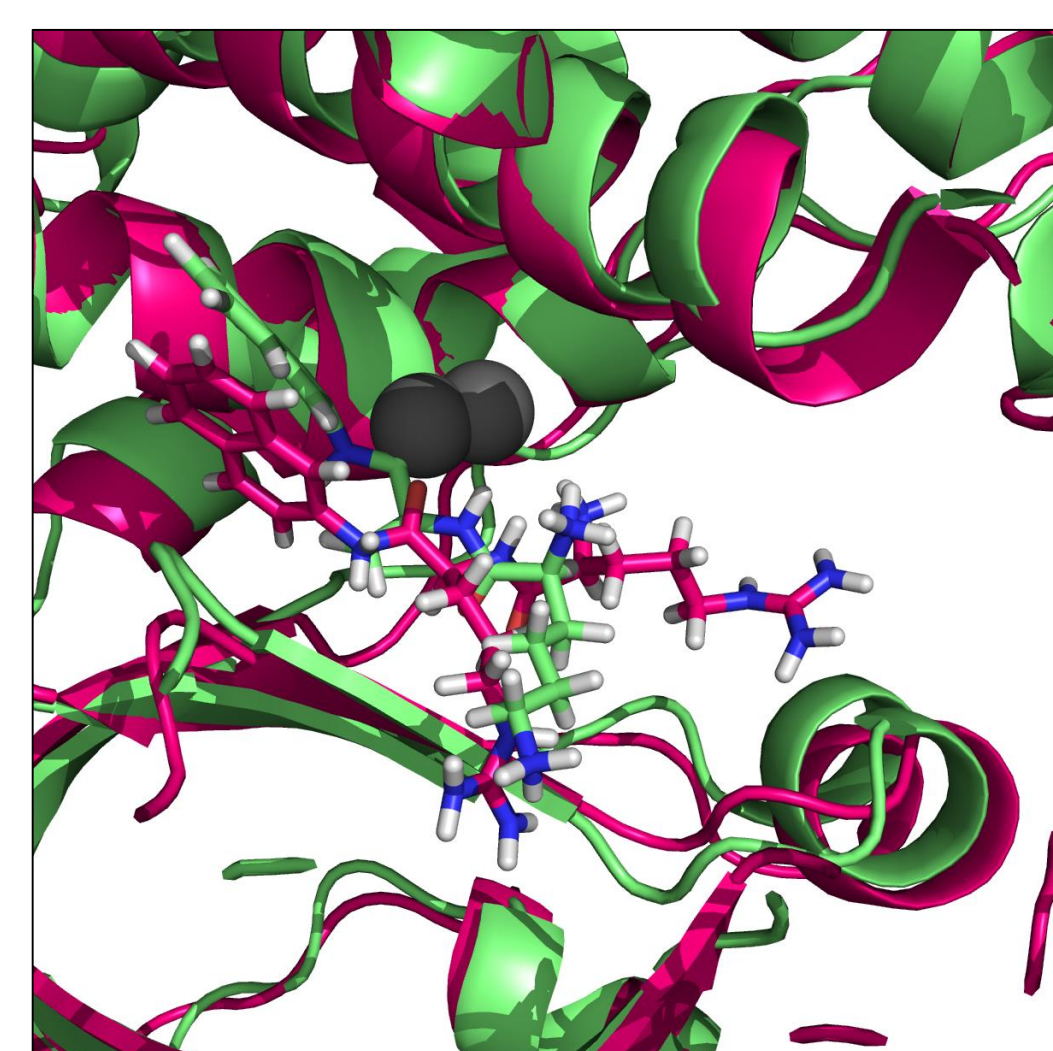


Figure 2. Comparison of active regions of the wild-type DPP III complexes with RRNA and KANA

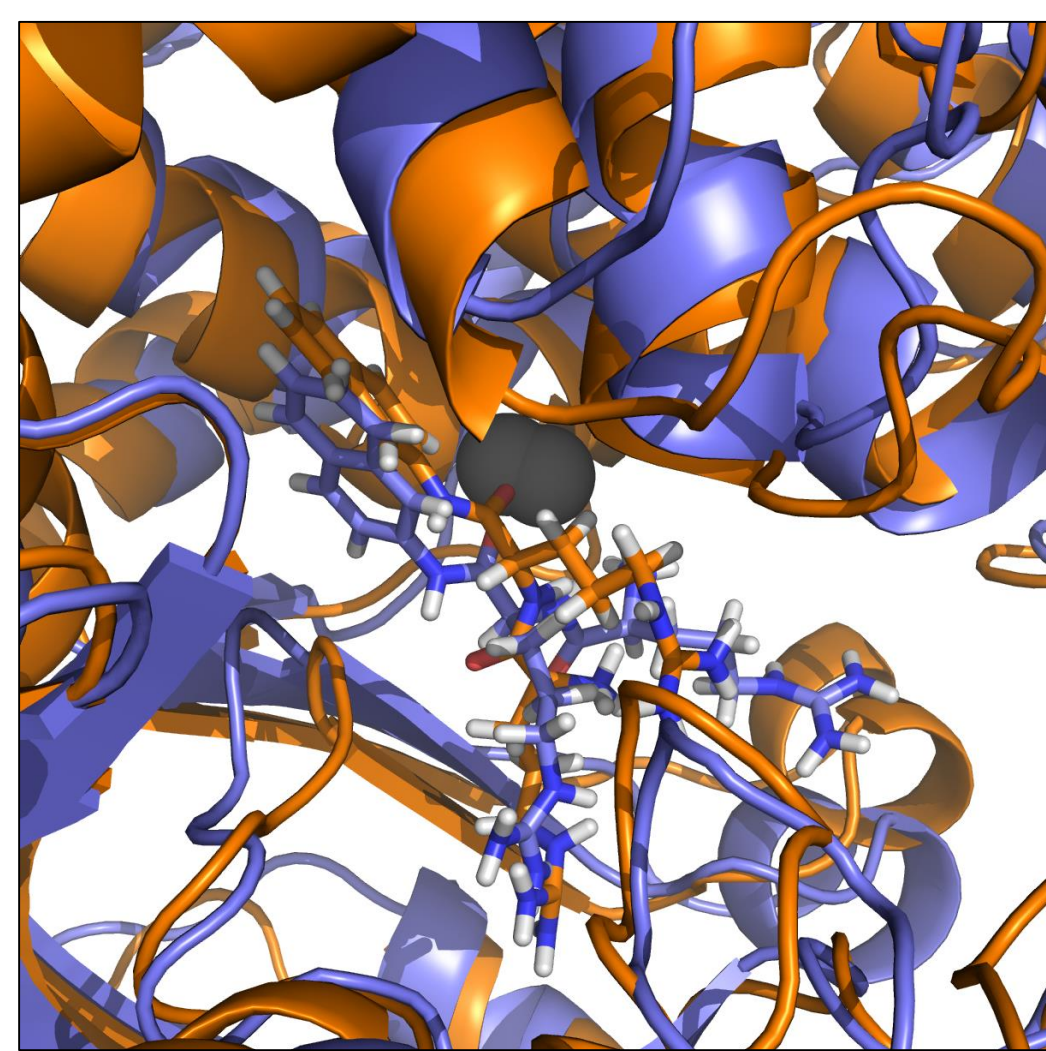


Figure 3. Comparison of active regions of the wild-type DPP III and the C450S mutant complex with RRNA

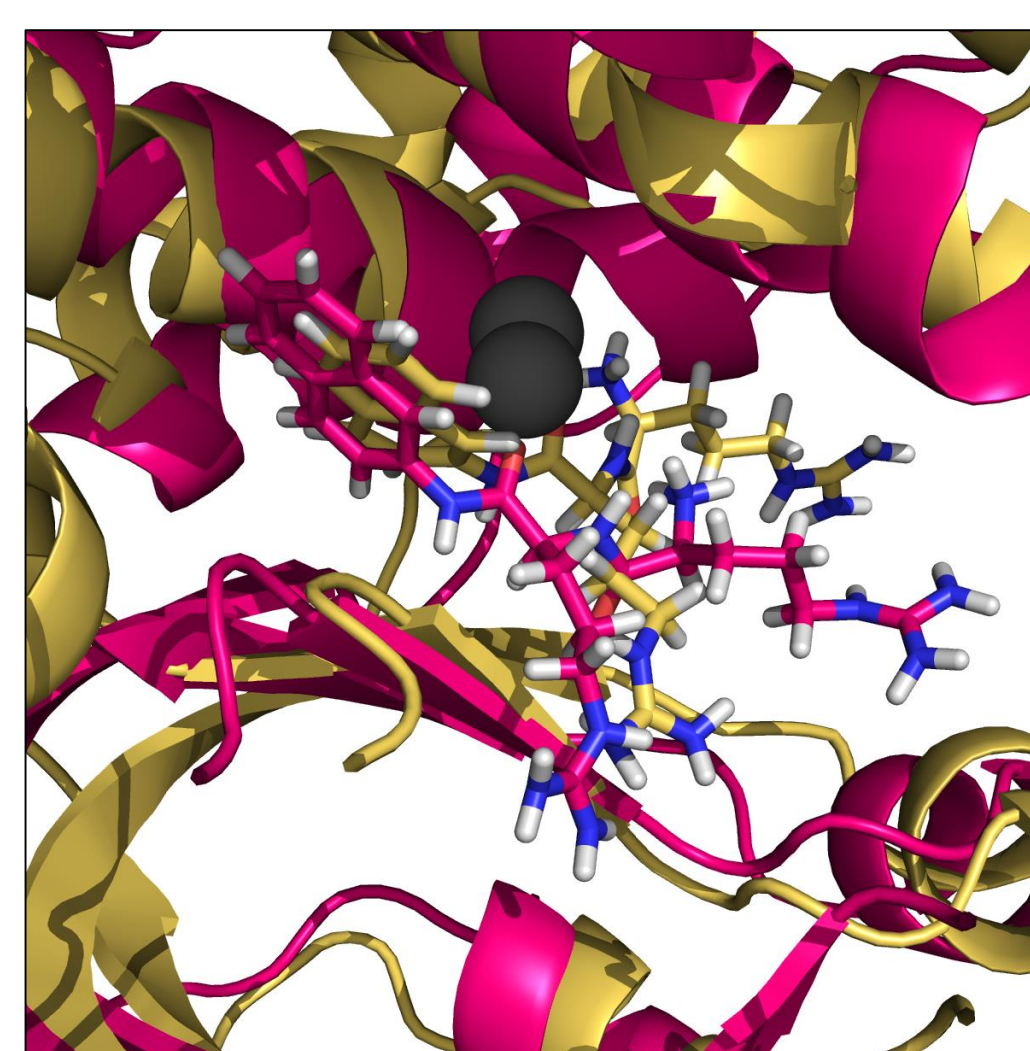


Figure 4. Overlap of the active sites with RRNA substrate in wild-type enzyme and the C450S mutant

Table 1. PB binding energies for DPPIII-RRNA and DPPIII-KANA complexes obtained by MM-PBSA

Complex	Method	$\Delta E_{pb}/\text{kcalmol}^{-1}$	Relative hydrolysis rate (%) <sup>3</sup>
DPPIII - RRNA	cMD/ff12SB	-49.76	100
DPPIII - RRNA	aMD/ff14SB	-57.83	
DPPIII - RRNA	aMD/ff14SB + cMD/ff12SB	-67.27	
DPPIII - KANA	cMD/ff12SB	-41.41	10.1
DPPIII - KANA	aMD/ff14SB	-35.33	
DPPIII - KANA	aMD/ff14SB + cMD/ff12SB	-47.68	

Table 2. PB binding energies for wild-type and C450S DPPIII-RRNA complex obtained by MM-PBSA

Complex	Method	$\Delta E_{pb}/\text{kcalmol}^{-1}$	$k_{cat}/\text{s}^{-1}$ <sup>3</sup>
wt-DPPIII	cMD/ff12SB	-49.76	5.0
wt-DPPIII	aMD/ff14SB	-57.83	
C450S DPPIII	cMD/ff12SB	-44.24	0.6
C450S DPPIII	aMD/ff14SB	-35.33	

## Hydrogen bond analysis

Table 3. Hydrogen bond analysis on lowest-energy 5ns fragments of docking trajectories. Only hydrogen bonds occurring in >30% of structures are shown

Acceptor	RRNA <sup>a</sup>	RRNA <sup>b</sup>	KANA <sup>a</sup>	KANA <sup>b</sup>
Glu307 (I)	31.08	43.88	47.48	-
Glu307 (II)	-	40.84	-	-
Glu320 (I)	70.88	59.44	-	-
Glu320 (II)	-	32.40	-	-
Asp375	-	-	38.88	-
Gly383	71.84	-	-	-
Glu476 (I)	98.72	35.08	66.76	97.56
Glu476 (II)	33.36	34.64	55.84	75.56
Glu476 (III)	-	33.24	31.28	-
Glu531	-	62.72	-	54.40

<sup>a</sup>Extracted from a 200ns ff12SB cMD simulation; <sup>b</sup>From a 100ns ff12SB simulation after 200ns of ff14SB aMD simulation

Table 4. Hydrogen bond analysis on lowest-energy 5ns fragments of RRNA docking trajectories

Acceptor	% of frames wt-DPPIII	% of frames C450S-DPPIII
Glu476 (I)	98.72	99.00
Gly383	71.84	14.44
Glu320	70.88	-
Glu476 (II)	33.36	21.60
Glu307	31.08	-
Glu449	-	77.84

## Conclusion

The 200 ns long MD simulations of the *Bacteroides thetaiotaomicron* DPP3 complexes with synthetic substrates RRNA and KANA revealed the long range interdomain movement consistent with the conformational changes determined for its human ortholog. Ff14 force field in conjunction with accelerated MD proved to be a fast and reliable docking method. Experimentally determined differences in hydrolysis rate of Arg<sub>2</sub>-naphtyl-2-amide and Lys-Ala-naphtyl-2-amide correlate with the substrates' potential for hydrogen bond formation. The importance of C450 has been explained through its influence on the substrate positioning, and the calculated complex energies are in qualitative agreement with experimental data. The residues found to stabilize the substrate via hydrogen bonds in our study are in agreement with the suggested subsites for *Bacteroides thetaiotaomicron* DPP III<sup>4</sup>.

Obtained structures will serve as a good starting point for future QM calculations aimed at unveiling the reaction mechanism of the peptide bond cleavage.

## References

1. A. Tomić, S. Tomić, *Dalton trans.* **43** (2014) 155503-155514.
2. D. Hamelberg, J. Mongan, J. A. McCammon, *J. Chem. Phys.* **120** (2004) 11919-11929.
3. B. Vukelić, B. Salopek-Sondi, J. Špoljarić, I. Sabljic, N. Meštrovic, D. Agic, M. Abramić, *Biol. Chem.* **393** (2012) 37-46.
4. A. Cvitešić, I. Sabljic, J. Makarević, M. Abramić, *J Enzyme Inhib Med Chem* 2016. DOI: 10.1080/14756366.2016.1186021